16th World Conference on Earthquake, 16WCEE 2017

Santiago Chile, January 9th to 13th 2017

Paper N° 670 (Abstract ID)

Registration Code: S-V1461989497

STUDY ON FEED-FORWARD CONTROL OF BASE-ISOLATED BUILDINGS USING SEISMIC INPUT MOTIONS

I. Nagashima[(1)] and R. Maseki[(2)]

[(1)] *Principal Research Engineer, Technology Center, Taisei Corporation, icniro.nagashima@sakura.taisei.co.jp*
[(2)] *Senior Research Engineer, Technology Center, Taisei Corporation, ryota.maseki@sakura.taisei.co.jp*
…

Abstract

This paper focuses on the use of feed-forward control techniques in base-isolated buildings to improve the control performance and efficiency of active response control systems for seismic excitations. Two approaches to feed-forward control are studied. One is optimal feedback and feed-forward control (FBFFC), which makes use of predicted earthquake ground motion before its arrival. The other is input cancellation control (ICC), which is directly derived to cancel the absolute displacement of a base-isolated building at every moment and does not require prediction of the input ground motion. FBFFC is derived as an optimal control problem formulated using absolute coordinates and a control algorithm is derived to reduce the absolute acceleration response.

It is found that the duration of the predicted seismic input motion required for FBFFC becomes shorter as control intensity increases, while control performance and the required control force approach those of ICC. Based on these findings, a new control algorithm that combines FBFFC and ICC is proposed. It is expected that this study will contribute to the development of a new approach to feed-forward active control of base isolated buildings.

Keywords: Active response control; Feed-forward Control; Base isolation; Optimal control theory

1. Introduction

Since the active mass driver system was first used in an actual Tokyo building in 1989 [1], there has been a steady increase in the number of buildings enhanced with active or semi-active response control systems in Japan. Active response control systems, and active mass damper systems in particular, have become firmly established as a technology that improves the habitability of super high-rise buildings during strong winds. Active response control systems are very effective. However, they use a feedback control law and are not suitable for fully controlling the seismic response of buildings due to limitations of control force and power. In other words, they are limited in application to earthquakes in the small to medium range.

This paper focuses on the use of feed-forward control techniques in base-isolated buildings to improve the control performance and efficiency of active response control systems during seismic excitations. Two approaches to feed-forward control are studied. One is optimal feedback and feed-forward control (FBFFC), which makes use of predicted ground motion before the arrival of an earthquake. The other is input cancellation control (ICC), which is directly derived to cancel the absolute displacement of a base-isolated building at every moment. With ICC, there is no need to predict the input ground motion.

FBFFC is derived as an optimal control problem formulated using an absolute coordinate system, and a control algorithm that reduces the absolute acceleration response is derived. An empirical transfer function for seismic waves between two points along the propagation path is used; one being the point of prediction (the location of the control system) and the other closer to the hypocenter of the earthquake being predicted. This transfer function, which is referred to as the prediction filter [2], is identified in the form of a state-space equation using past earthquake observations and is then used for the real-time prediction of future ground motions. A control algorithm that uses such predicted ground motions, of limited duration amounting to several times the natural period of the base-isolated building, has been already presented [3]. In this work, the relation between the required duration of the predicted input motion and the intensity of the active FBFFC is further studied and compared with the ICC in analysis in both the frequency domain as well as the time domain.

It is found that the duration of the predicted seismic input motion required by FBFFC becomes shorter as control intensity increases, and the control performance and required control force approach the ICC results. Based on these findings, a new control algorithm that combines FBFFC with ICC is presented. It is expected that this study will contribute to developing a new approach to feed-forward active control of base isolated buildings.

2. Linear regulator problems with external excitations [4]

2.1 Optimal feedback and feed-forward control

In an absolute coordinate system, the state equations and the evaluation function for the objects to be controlled are given by the equations provided below.

$$\dot{\mathbf{x}}(\mathrm{t}) = \mathbf{A}\mathbf{x}(t) + \mathbf{B}\mathbf{u}(t) + \mathbf{E}\mathbf{y}_0(t) \tag{1}$$

where $\mathbf{A}$ and $\mathbf{B}$ are $\mathrm{n}\times\mathrm{n}$ and $\mathrm{n}\times\mathrm{m}$ constant matrices, $\mathbf{x}(t)$ is the state vector, $\mathbf{u}(t)$ is the control input vector, and $\mathbf{y}_0(t)$ is obtained by combining the displacement and velocity of the input seismic motion.

The performance measure to be minimized is

$$\mathbf{J} = \frac{1}{2}\int_0^{t_f} \left\{ \mathbf{x}^{\mathrm{T}}(t)\mathbf{Q}\mathbf{x}(t) + \mathbf{u}^T(t)\mathbf{R}\mathbf{u}(t) \right\} dt \tag{2}$$

where $\mathbf{Q}$ is a real symmetric positive semi-definite matrix and $\mathbf{R}$ is real symmetric and positive definite. The final time t_f is fixed, $\mathbf{x}(t_f)$ is free, and the states and controls are not bounded.

The Hamiltonian is given by

$$H(\mathbf{x}(t), \mathbf{u}(t), \mathbf{p}(t), t) = \frac{1}{2}\left[\mathbf{x}^{\mathrm{T}}(t)\mathbf{Q}\mathbf{x}(t) + \mathbf{u}^T(t)\mathbf{R}\mathbf{u}(t)\right] + \mathbf{p}^{\mathrm{T}}(t)\left[\mathbf{A}\mathbf{x}(t) + \mathbf{B}\mathbf{u}(t) + \mathbf{E}\mathbf{y}_0(t)\right]. \tag{3}$$

The costate equations are

$$\dot{\mathbf{p}}(t) = -\frac{\partial H}{\partial \mathbf{x}} = -\mathbf{Q}\mathbf{x}(t) - \mathbf{A}^{\mathrm{T}}\mathbf{p}(t) \tag{4}$$

and the algebraic relations that must be satisfied are given by

$$\mathbf{0} = \frac{\partial H}{\partial \mathbf{u}} = \mathbf{R}\mathbf{u}(t) + \mathbf{B}^{\mathrm{T}}\mathbf{p}(t)\,; \tag{5}$$

Therefore,

$$\mathbf{u}(t) = -\mathbf{R}^{-1}\mathbf{B}^{\mathrm{T}}\mathbf{p}(t) \tag{6}$$

Let us assume that the costate is expressed by the equation

$$\mathbf{p}(t) = \mathbf{K}(t)\mathbf{x}(t) + \mathbf{s}(t) \tag{7}$$

Differentiating both sides with respect to t, we obtain

$$\dot{\mathbf{p}}(t) = \dot{\mathbf{K}}(t)\mathbf{x}(t) + \mathbf{K}(t)\mathbf{x}(t) + \dot{\mathbf{s}}(t)\,.$$

Substituting from Eq. (4) for $\dot{\mathbf{p}}(t)$, and Eq. (1) for $\dot{\mathbf{x}}(t)$, and using Eq. (7) to eliminate $\mathbf{p}(t)$, we obtain

$$\left[\dot{\mathbf{K}}(t) + \mathbf{Q} + \mathbf{K}(t)\mathbf{A} + \mathbf{A}^{\mathrm{T}}\mathbf{K}(t) - \mathbf{K}(t)\mathbf{B}\mathbf{R}^{-1}(t)\mathbf{B}^{T}\mathbf{K}(t)\right]\mathbf{x}(t) + \left[\mathbf{s}(t) + \mathbf{A}\mathbf{s}(t) - \mathbf{K}(t)\mathbf{B}\mathbf{R}^{-1}\mathbf{B}^{\mathrm{T}}\mathbf{s}(t) + \mathbf{K}(t)\mathbf{E}\mathbf{y}_0(t)\right] = \mathbf{0} \tag{8}$$

Because this must be satisfied for all $\mathbf{x}(t)$ and $\mathbf{s}(t)$, we obtain

$$\dot{\mathbf{K}}(t) = -\mathbf{K}(t)\mathbf{A} - \mathbf{A}^{T}\mathbf{K}(t) - \mathbf{Q} + \mathbf{K}(t)\mathbf{B}\mathbf{R}^{-1}\mathbf{B}\mathbf{K}(t) \tag{9}$$

and

$$\dot{\mathbf{s}}(t) = -\left[\mathbf{A}^{T} - \mathbf{K}(t)\mathbf{B}\mathbf{R}^{-1}\mathbf{B}\right]\mathbf{s}(t) - \mathbf{K}(t)\mathbf{E}\mathbf{y}_0(t) \tag{10}$$

To obtain the boundary conditions we have, from Eq. (7),

$$\mathbf{p}(t_f) = \mathbf{K}(t_f)\mathbf{x}(t_f) + \mathbf{s}(t_f) = \mathbf{0}\,. \tag{11}$$

Since this equation must be satisfied for all $\mathbf{x}(t_f)$, the boundary conditions are

$$\mathbf{K}(t_f) = \mathbf{0}\text{, and } \mathbf{s}(t_f) = \mathbf{0} \tag{12}$$

In the following study, a constant matrix $\mathbf{K}$, which is obtained for an infinite-time process as $t_f \to \infty$, is used to determine the feedback control force. The $\mathbf{K}$ matrix is obtained by solving the algebraic matrix Riccati equation

$$\mathbf{0} = -\mathbf{K}\mathbf{A} - \mathbf{A}^{T}\mathbf{K} - \mathbf{Q} + \mathbf{K}\mathbf{B}\mathbf{R}^{-1}\mathbf{B}^{T}\mathbf{K}\,, \tag{13}$$

obtained by setting $\dot{\mathbf{K}}(t) = \mathbf{0}$ in Eq. (9).

The optimal feedback and feed-forward control force is the sum of the optimal feedback control force $\mathbf{u}_{fb}(t)$ ($= -\mathbf{R}^{-1}\mathbf{B}^{T}\mathbf{K}x(t)$) and the optimal feed-forward control force $\mathbf{u}_{ff}(t)$ ($= -\mathbf{R}^{-1}\mathbf{B}^{T}\mathbf{s}(t)$);

$$\mathbf{u}(t) = \mathbf{u}_{fb}(t) + \mathbf{u}_{ff}(t) = -\mathbf{R}^{-1}\mathbf{B}^{T}\mathbf{K}\mathbf{x}(t) - \mathbf{R}^{-1}\mathbf{B}^{T}\mathbf{s}(t)\,. \tag{14}$$

Substituting Eq. (14) into Eq. (1), we obtain

$$\dot{\mathbf{x}}(t) = \mathbf{A}_c\mathbf{x}(t) + \mathbf{F}\mathbf{s}(t) + \mathbf{E}\mathbf{y}_0(t)\,, \tag{15}$$

where $\mathbf{F} = -\mathbf{R}^{-1}\mathbf{B}$ and $\mathbf{A}_c = \mathbf{A} - \mathbf{R}^{-1}\mathbf{B}^{T}\mathbf{K}$.

The state space equation for $\mathbf{s}(t)$, which determines the feed-forward control force, is expressed by

$$\dot{\mathbf{s}}(t) = -\mathbf{A}_c{}^{\mathrm{T}}\mathbf{s}(t) - \mathbf{KEy}_0(t)\,. \tag{16}$$

To predict the input base excitations, $\mathbf{y}_0(t)$, we introduce the following identified state space equations, named the prediction filter [2].

$$\dot{\mathbf{z}}_d(t) = \mathbf{A_d z_d}(t) + \mathbf{D_d}\ddot{\mathbf{w}}(t)\,, \qquad \mathbf{y}_0(t) = \mathbf{C}_d\mathbf{z}_d(t)\,, \tag{17}$$

where $\ddot{\mathbf{w}}(t)$ is the input acceleration to the prediction filter.

Once $\mathbf{y}_0(t)$ is predicted with the help of Eq. (17), the optimal feed-forward control force may be calculated by integrating Eq. (16) backward in time starting from $t = t_f$. It was generally believed that the whole time history of the input base accelerations should be known beforehand to determine the feed-forward control force. Various control algorithms using predicted base accelerations of limited duration have been developed [3] and will be reviewed in the following section.

To study the frequency response characteristics of FBFFC with respect to the input accelerations to the prediction filter, the extended state space equation is defined from Eqs. (15), (16) and (17) as follows:

$$\begin{pmatrix} \dot{\mathbf{x}}(t) \\ \dot{\mathbf{s}}(t) \\ \dot{\mathbf{z}}_d(t) \end{pmatrix} = \begin{bmatrix} \mathbf{A}_c & \mathbf{F} & \mathbf{EC}_d \\ \mathbf{0} & -\mathbf{A}_c{}^T & \mathbf{KEC}_d \\ \mathbf{0} & \mathbf{0} & \mathbf{D}_d \end{bmatrix} \begin{pmatrix} \mathbf{x}(t) \\ \mathbf{s}(t) \\ \mathbf{z}_d(t) \end{pmatrix} + \begin{pmatrix} \mathbf{0} \\ \mathbf{0} \\ \mathbf{D}_d \end{pmatrix} \ddot{\mathbf{w}}(t) \tag{18}$$

3. Active response control algorithms considering external excitations

To evaluate the optimal feed-forward control force in the time domain, it is necessary in general to know the whole time history of ground base acceleration in advance [5]. A control algorithm that uses the free vibration component, which can be predicted in advance, has previously been presented as a way to evaluate the feed-forward control force [6]. A control algorithm that uses input accelerations of limited duration has been devised based on the dynamic programming approach [7]. However, there appears to be no fully developed practical control algorithm for determining the feed-forward control force in the time domain. In the sections that follow, an optimal feed-forward control that uses the whole time history is first described. Then a practical control algorithm that approximates the optimal feed-forward control force based on a limited part of the full base acceleration history is explained [3].

3.1 Optimal feed-forward control with global optimization

The impulse response function of the feed-forward control force may be calculated backward in time starting from $t = t_f$ using Eq. (16). Let us assume that the transition matrix of the state space equation (16) is $\mathbf{\Phi}(t)$. The impulse response function $\mathbf{h}(t)$, which is an anti-causal function, is then obtained by

$$\left.\begin{aligned} &\mathbf{h}(t) = \mathbf{0} && \textit{for} \quad t > 0 \\ &\mathbf{h}(t) = -\mathbf{\Phi}(t)\mathbf{KE}\{1\} && \textit{for} \quad t \le 0 \end{aligned}\right\}, \tag{19}$$

where $\mathbf{\Phi}(t)$ is calculated from the inverse Laplace transform of the transfer function $(s\mathbf{I} + \mathbf{A}_c{}^T)^{-1}$.

The feed-forward control force at time t may be given by

$$\mathbf{u}_{ff}(t) = -\mathbf{R}^{-1}\mathbf{B}^T\mathbf{s}(t_f - t)\,, \tag{20}$$

where $\mathbf{s}(t)$ is calculated backward in time using the following equation,

$$\mathbf{s}(t_f - t) = \mathbf{\Phi}(t - t_f)\cdot\mathbf{s}(t_f) - \int_{t_f}^{t}\mathbf{h}(t_f - \tau)\mathbf{y}_0(\tau)d\tau\,.\ \ t_f \ge t \ge 0 \tag{21}$$

The second term on the right-hand side of (21) is a convolution integral. Assuming the boundary condition $\mathbf{s}(t_f) = \mathbf{0}$, Eq. (21) can be simplified as

$$\mathbf{s}(t_f - t) = -\int_{t_f}^{t} \mathbf{h}(t_f - \tau)\mathbf{y}_0(\tau)d\tau \tag{22}$$

As is clear from Eq. (22), the full time history of the ground base acceleration from t_f to t must be known in advance to determine the feed-forward control force at t.

Let us divide the time history of ground base acceleration into N blocks with each interval endpoint denoted by $t_i, (i = 1,...,N)$.

The feed-forward control force for the i-th block may be calculated by

$$\mathbf{u}_{ffi}(t) = -\mathbf{R}^{-1}\mathbf{B}^T\mathbf{s}(t_i - t) \tag{23}$$

where $\mathbf{s}(t_i - t)$ is evaluated, following (21) and (22), as

$$\mathbf{s}(t_i - t) = \mathbf{\Phi}(t - t_i)\cdot\mathbf{s}(t_f - t_i) - \int_{t_i}^{t} \mathbf{h}(t_i - \tau)\mathbf{y}_0(\tau)d\tau \qquad t_i \geq t \geq t_{i-1} \tag{24}$$

and

$$\mathbf{s}(t_f - t_i) = -\int_{t_f}^{t_i} \mathbf{h}(t_f - \tau)\mathbf{y}_0(\tau)d\tau \tag{25}$$

The feed-forward control force for the i-th block is determined by (23), which we call feed-forward control by global optimization (GFFC).

3.2 Optimal feed-forward control with modified individual optimization

Next, let us consider the following individual performance measure:

$$\mathbf{J}_i = \frac{1}{2}\int_{t_{i-1}}^{t_i} \left\{\mathbf{x}^{\mathrm{T}}(t)\mathbf{Q}\mathbf{x}(t) + \mathbf{u}^T(t)\mathbf{R}\mathbf{u}(t)\right\}dt, \tag{26}$$

where the ground base acceleration is assumed to be zero after t_i (or the boundary condition $\mathbf{s}(t_i) = \mathbf{0}$ is assumed). The optimal feed-forward control force for the i-th block may be calculated using (22):

$$\hat{\mathbf{u}}_{ffi}(t) = -\mathbf{R}^{-1}\mathbf{B}^T\hat{\mathbf{s}}(t_i - t), \tag{27}$$

where

$$\hat{\mathbf{s}}(t_i - t) = -\int_{t_i}^{t} \mathbf{h}(t_i - \tau)\mathbf{y}_0(\tau)d\tau \qquad t_i \geq t \geq t_{i-1}. \tag{28}$$

The feed-forward control force for the i-th block is determined by (27), which we call feed-forward control by individual optimization (IFFC). The GFFC is expected to perform better than the IFFC, due to the effect of the first term on the right-hand side of Eq. (24), i.e. the homogeneous solution, which, however may be negligible as long as $|t - t_i|$ is sufficiently large that the transition matrix $\mathbf{\Phi}(t - t_i)$ approaches $\mathbf{0}$.

If the homogeneous solution becomes small enough with $t_i - t \geq T_d$ and the ground base acceleration can be predicted for more than $T_d + T_a$ seconds in advance, the IFFC value of $\hat{\mathbf{u}}_{ffi}(t)$ may approximate to the GFFC $\mathbf{u}_{ffi}(t)$ for t ranging between t_{i-1} and $t_{i-1} + T_a$. Using this principle, a control algorithm that improves the performance of IFFC is devised, as shown in Fig. 1, where the IFFC value of $\hat{\mathbf{u}}_{ffi}(t)$ for the coming $T_d + T_a$ seconds is calculated at $t = t_{i-1}$ and is used for T_a seconds; the IFFC value of $\hat{\mathbf{u}}_{ffi+1}(t)$ for the coming $T_d + T_a$ seconds is then calculated at $t = t_i (= t_{i-1} + T_a)$ and again used for T_a seconds. This procedure is iterated to determine the feed-forward control forces, in a process that we call feed-forward control by modified individual optimization (MIFFC).

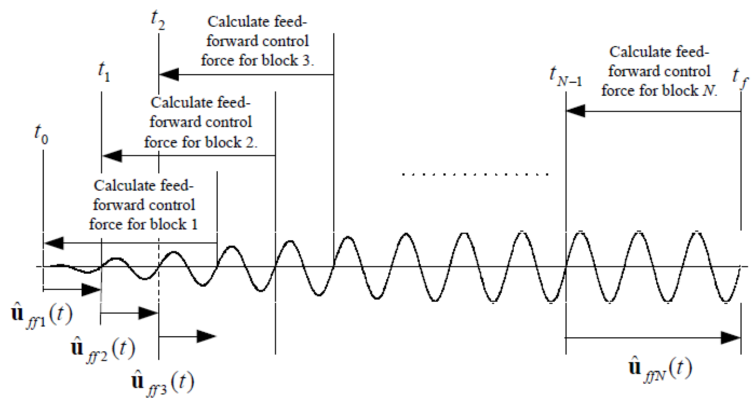

Fig. 1 Schematic for determining the feed-forward control force for MIFFC

3.3 Seismic input cancellation control

In control that absorbs the movement of the seismic motions in a base isolation layer with low stiffness, the third term of Eq. (1) may be canceled out by the second term of the control force [8]. This control is referred to as Input Cancellation Control (ICC). The control force u is obtained from the following equation in case of uni-directional control:

$$\mathrm{u} = \mathrm{k}\,\mathrm{y}_0 + \mathrm{c}\,\dot{\mathrm{y}}_0 \tag{29}$$

where k is the stiffness of the base isolation layer, c is the damping coefficient and y_0 and $\dot{\mathrm{y}}_0$ are the displacement and velocity of the input seismic motion, respectively.

4. Feed-forward control of base-isolated building

Let us consider a single-degree-of-freedom building model, as shown in Fig.2. The mass, the stiffness, and the natural circular frequency of the building model are denoted by m_s, k_s, ω_s, respectively. The damping coefficient and the corresponding damping factor are denoted by c_s and ζ_s. The absolute displacement of the structure is denoted by x_s. The scalar control force and the ground base excitation are given by $u(t)$ and $y_0(t)$, respectively.

The state space equations are given by Eq. (1), where $\mathbf{x}(t) = \left(x_s(t), \quad \dot{x}_s(t)\right)$,

$$\mathbf{A} = \begin{bmatrix} 0 & 1 \\ -\omega_s^2 & -2\zeta_s\omega_s \end{bmatrix}, \quad \mathbf{B} = \begin{bmatrix} 0 \\ m_s^{-1} \end{bmatrix}, \quad \mathbf{E} = \begin{bmatrix} 0 \\ -1 \end{bmatrix}, \quad \omega_s = \sqrt{\frac{k_s}{m_s}}, \quad \zeta_s = \frac{c_s}{2m_s\omega_s} \tag{30}$$

The performance measure is given by Eq. (2), where

$$\mathbf{Q} = \begin{bmatrix} q_d & \\ & q_v \end{bmatrix}, \qquad \mathbf{R} = [r] \tag{31}$$

The solutions of the matrix Reccati equations are given by $\mathbf{K} = \begin{bmatrix} k_{11} & k_{12} \\ k_{12} & k_{22} \end{bmatrix}$,

where $k_{11} = 2\zeta_s\omega_s k_{12} + \omega_s^2 k_{22} + k_{12}k_{22}/(m_s^2 r)$, $k_{12} = -m_s^2 r\omega_s^2 + \sqrt{m_s^4 r^2\omega_s^4 + m_s^2 r q_1}$ and

$k_{22} = -2m_s^2 r\zeta_s\omega_s + \sqrt{4m_s^4 r^2\zeta_s^2\omega_s^2 + (2k_{12} + q_2)m_s^2 r}$

Next, the prediction filter in this study is simplified as a band pass filter, of which the transfer function is

$$\frac{\ddot{z}_0(s)}{\ddot{w}(s)} = \frac{\omega_d{}^2}{s^2 + 2\zeta_d \omega_d s + \omega_d{}^2} \cdot \frac{s^2}{s^2 + 2\zeta_h \omega_h s + \omega_h{}^2}. \tag{32}$$

The corresponding state space equation is given by Eq. (17), where

$$\mathbf{A}_d = \begin{bmatrix} 0 & 1 & 0 & 0 \\ 0 & 0 & 1 & 0 \\ 0 & 0 & 0 & 1 \\ -a & -b & -c & -d \end{bmatrix}, \ \mathbf{D}_d = \begin{bmatrix} 0 \\ 0 \\ 0 \\ \omega_d{}^2 \end{bmatrix}, \ \mathbf{C}_d = \begin{bmatrix} 0 \\ 0 \\ 1 \\ 0 \end{bmatrix}^T, \ \mathbf{z}_d = \begin{bmatrix} z_0 \\ \dot{z}_0 \\ \ddot{z}_0 \\ \dddot{z}_0 \end{bmatrix} \tag{33}$$

$$a = \omega_d{}^2 \omega_h{}^2, \ b = 2\omega_d \omega_h (\zeta_d \omega_h + \zeta_h \omega_d), \ c = \omega_d{}^2 + 4\zeta_d \zeta_h \omega_d \omega_h + \omega_h{}^2, \ d = 2(\zeta_h \omega_h + \zeta_d \omega_d).$$

The parameters for the building model are as follows: the natural period of the building is 0.25s and the corresponding natural circular frequency $\omega_s = 2\pi / 0.25$ rad/s, ζ_s =0.10, and $m_s = 1.0 \times 10^6$ kg. The parameters for the prediction filter are; $\omega_h = \omega_s / 10$, $\zeta_h = 0.70$, $\omega_d = 10 \times \omega_s$, and $\zeta_d = 0.707$. Fig. 3 shows the frequency response function of the prediction filter.

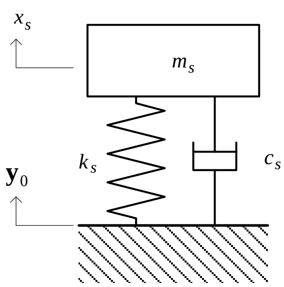

Fig. 2 A single-degree-of-freedom building model

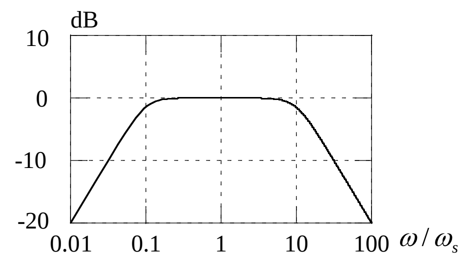

Fig. 3 Frequency response function of prediction filter

4.1 Optimal feedback and feedforward control

4.1.1 Control performance in frequency domain

The frequency responses of the optimal feedback and feed-forward control (FBFFC), as well as those of the optimal feedback control (FBC), with respect to the input acceleration $\ddot{w}(i\omega)$ are calculated from the Fourier transform of Eq. (18). Figure 4(a) shows the frequency responses of the building acceleration per unit input acceleration with the FBC. The dimensionless weighting parameters for the control are defined as r, $\overline{q}_d = q_d /(m_s{}^2 \omega_s{}^4 r)$, and $\overline{q}_v = q_v /(m_s{}^2 \omega_s{}^2 r)$. The frequency responses are calculated for increasing $\overline{q}_d = \overline{q}_v =$ 0.2, 0.5, 2.0, and 6.0 with $r =$ 1.0 fixed. The equivalent modal damping factors increase as 31%, 44%, 71%, and 93% in accordance with the respective weighting coefficients. The corresponding frequency responses of the control force normalized by the building mass are shown in Fig. 4(b). The frequency response of the ICC control force given by Eq. (29) is also illustrated by the solid red line. The ICC control force seems to envelop the frequency response of the FBC control force. In the low-frequency region below the natural frequency, the control force increases rapidly. The FBFFC results are shown in Fig. 5. The control force is lower above the natural frequency, while the acceleration response is remarkably reduced at and below the natural frequency. In particular there is a significant reduction in acceleration response in the vicinity of the natural frequency, confirming the effectiveness of feed-forward control in reducing resonance response. Note that in this case also the ICC control force is shown as the envelope frequency response of the FBFFC control force.

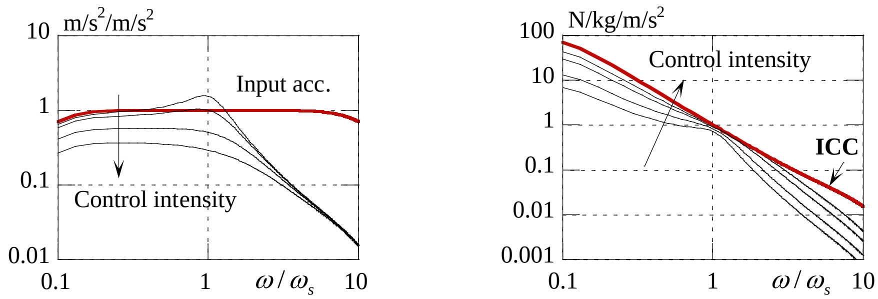

(a) Acceleration response (b) Control force

Fig. 4 Comparison of frequency response (FBC)

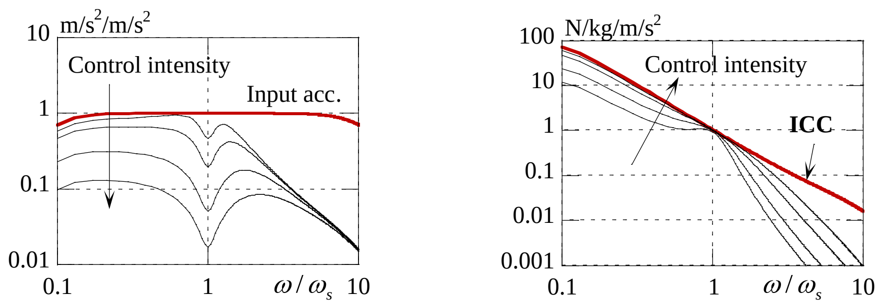

(a) Acceleration response (b) Control force

Fig. 5 Comparison of frequency response (FBFFC)

4.1.2 Control performance in time domain

The time domain performance of FBFFC and ICC are compared in this section. The NS component of the El Centro 1940 waveform is used as the seismic input acceleration for the prediction filter, Eq. (18). The maximum filtered acceleration is normalized to 1.0m/s^2. The time history of the FBFFC force and acceleration response for the weighting coefficients ($\bar{q}_d = \bar{q}_v$ = 2.0 and 6.0) are plotted and compared with ICC in Fig. 6. The time delay of the control force due to the sampling time interval of 0.005s is considered in ICC. ICC performs better than any other FBFFC at the cost of larger control force. The ICC control force seems to be obtained as the limit case of FBFFC control force.

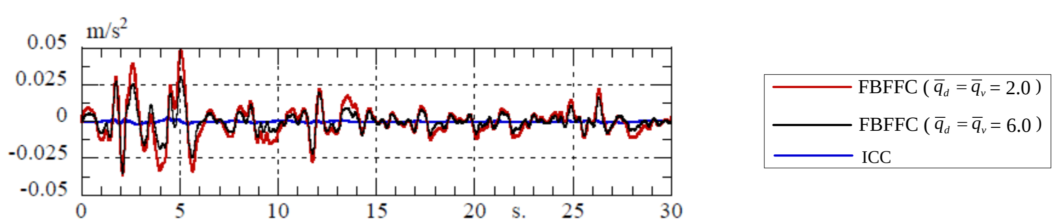

(a) Acceleration response

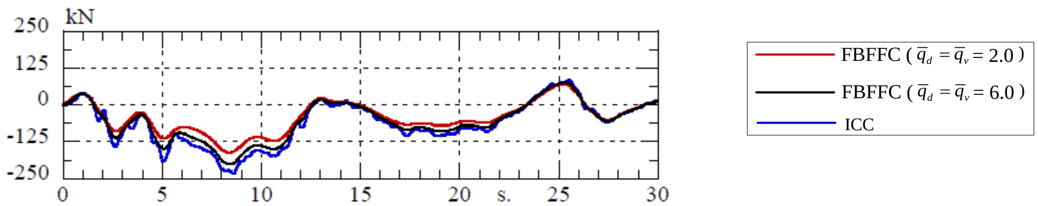

(b) Control force

Fig. 6 Comparison of time history response

4.2 Development of feedback and input cancellation control

The results obtained in Section 4.1 indicate that ICC may be obtained as the limit case of FBFFC. To implement feed-forward control, some duration of predicted seismic input excitation is generally required for MIFFC, as explained in Section 3.2. However, as the control intensity increases, the required duration of the prediction may be reduced as investigated in the following.

To calculate the feed-forward control force for the analyses model, the transition matrix of the state space of Eq. (16) is expressed as

$$\mathbf{\Phi}(t) = e^{h_c\omega_c t}\begin{bmatrix} \cos\alpha t - \dfrac{h_c\omega_c}{\alpha}\sin\alpha t & \dfrac{\omega_c^{\,2}}{\alpha}\sin\alpha t \\ -\dfrac{1}{\alpha}\sin\alpha t & \cos\alpha t + \dfrac{h_c\omega_c}{\alpha}\sin\alpha t \end{bmatrix} \tag{34}$$

where $\alpha = \omega_c\sqrt{1-h_c^{\,2}}$, $\omega_c^{\,2} = \omega_s^{\,2} + \dfrac{k_{12}}{m_s^{\,2} r}$ and $2h_c\omega_c = 2h_s\omega_s + \dfrac{k_{22}}{m_s^{\,2} r}$.

The value of $h_c\omega_c$ in Eq. (34) increases to infinity as the control intensity increases. The feed-forward control force for the ***i***-th time block is expressed by Eq. (24) and the homogeneous solution may become negligible immediately because the transition matrix $\mathbf{\Phi}(t-t_i)$ approaches **0** for $t<t_i$. The impulse response function $\mathbf{h}(t)$ expressed by Eq. (19) would increase at $t=t_i$. However, it would also converge to zero immediately for $t<t_i$. Thus ICC may be obtained as the limit case of FBFFC.

The performance of ICC is extreme because the input seismic excitation is cancelled. However, the required control force may become very large. On the other hand, ICC has the great advantage that it does not require prediction of the seismic motion.

ICC could be used to cancel a part of the seismic input and combined with FBC. This method of control is referred to as feedback and input cancellation control (FBICC). Figure 7 shows the results of FBICC in which the input was reduced by 50% using ICC and then combined with FBC ($\bar{q}_d = \bar{q}_v$ = 2.0). The results obtained with FBC and FBFFC for the weighting coefficient ($\bar{q}_d = \bar{q}_v$ = 2.0) are also plotted in Fig. 7. FBICC improves control performance of FBC over the whole frequency range. Particularly in the range above the natural frequency, such an improvement is not attainable by FBC only, as indicated in Fig. 4. The required control force with FBICC, however, is more than that of both FBC and FBFFC, but is less than that of ICC.

As noted above, FBFFC is remarkably effective at reducing the resonance response. If predictions of seismic motion are available, FBFFC should be used so as to reduce the resonance response effectively. In other cases, FBICC may be used to improve on the control performance of FBC. ICC may be used to achieve the best performance if the control force required to cancel 100% of the seismic input is available.

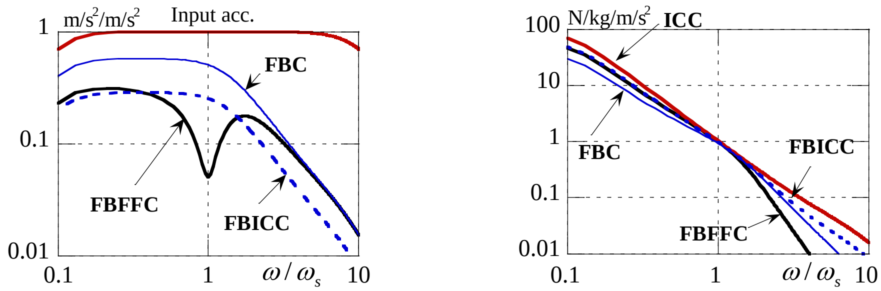

(a) Acceleration response (b) Control force

Fig. 7 Comparison of frequency response (FBC, FBFFC and FBICC)

The time domain performance of FBICC is compared with FBC and FBFFC for the weighting coefficients ($\bar{q}_d = \bar{q}_v$ = 2.0) in Fig. 8. The NS component of the El Centro 1940 waveform is used as the seismic input acceleration for the prediction filter, Eq. (18). The maximum filtered acceleration is normalized to 1.0m/s^2. The input excitation for FBICC was reduced by 50% by ICC and then combined with FBC ($\bar{q}_d = \bar{q}_v$ = 2.0). FBICC performs better than FBC and achieves almost the same performance as FBFFC.

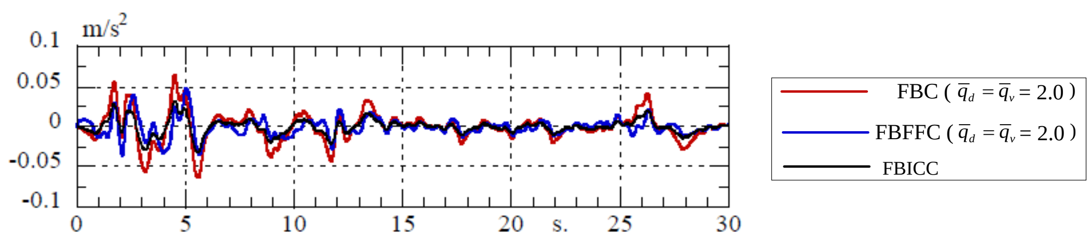

(a) Acceleration response

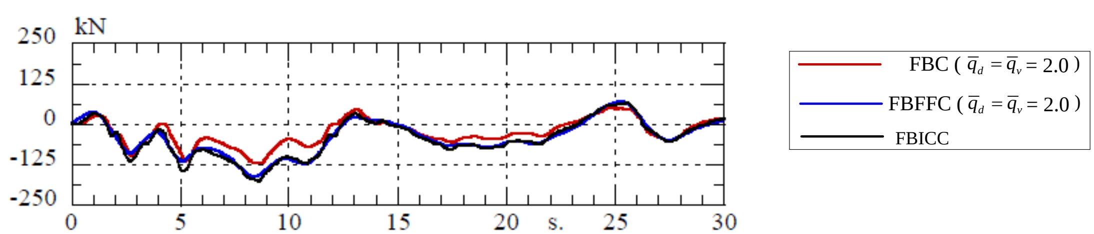

(b) Control force

Fig. 8 Comparison of time history response

5. Conclusions

As control intensity increases, the duration of the predicted seismic motion that is required as an input by feedback and feed-forward control (FBFFC) becomes shorter, while the control performance and required control force approach those of input cancellation control (ICC). Based on this finding, a feedback and input cancellation control (FBICC) algorithm that combines feedback control (FBC) and ICC is proposed. The control force required for FBICC may be larger than for FBC and for FBFFC, but is smaller than required for ICC. The great advantage with FBICC is that the prediction of seismic input excitation is not needed. If predictions of seismic motion are available, FBFFC should be used to reduce resonance response effectively. Otherwise, FBICC may be used to improve the control performance of FBC. ICC achieves the best performance if sufficient control force required to completely cancel the seismic input is available. It is expected that this study will contribute to the development of a new approach to feed-forward active control of base isolated buildings.

6. Acknowledgements

This research was carried out with financial assistance, with partial support from JSPS KAKENHI(C) (25420604) (research representative: Ichiro Nagashima).

7. References

[1] Kobori, T, Koshika, N, Yamada, K. and Ikeda, Y. (1991): Seismic-response-controlled structure with active mass driver system. Part 1: design. *Earthquake Engng. Struct. Dyn.* **20**, 133-149.

[2] Nagashima I. Yoshimura C. Uchiyama Y. Maseki R. and Itoi T. (2008): Real-time prediction of earthquake ground motion using empirical transfer function. *Proc. of 14th WCEE,* **S02-023**.

[3] Nagashima, I. and Maseki, R. (2012): Study on feed-forward control of base-isolated buildings using predicted propagation of seismic waves, *Proc. of 15th* WCEE, Lisboa.

[4] Kirk, D. E. (2004): Optimal control theory, an introduction, Dover Publications, Inc. Mineola, New York.

[5] Sato Y., Ishimaru, S. and Miwa, S. (1989): Comparative study for control algorithm of SDOF structures, Part II On procedures for tracking problems, AIJ annual meeting, 549-550. (in Japanese)

[6] Naraoka K. and Katukura, H. (1992): A study on feedback-feedforward control algorithm which utilizes information of future input, J. Struct. Constr. Eng., AIJ, No.438, 75-81. (in Japanese).

[7] Kawahara, M. and Fukazawa, K. (1989): Optimal control of structure subject to earthquake loading using dynamic programming, Proc. of JSCE, No.404/i-11, 179-190.

[8] Minoru Kageyama et al.(1989): Research into Vibration Control of Structures (Part 5) Theoretical Study of Absolute Vibrations of Multi-layer Structures, Summaries of Technical Papers of the Annual Meeting of the Architectural Institute of Japan. (in Japanese)